Research Article

C. Anil Kumar Reddy*, Pothamsetty Kasi V. Rao, Begori Venkatesh and Boggarapu Nageswara Rao

Influence of gas nitriding on the surface layer of M50 NiL steel for aerospace-bearing applications

https://doi.org/10.1515/jmbm-2024-0030
received August 30, 2024; accepted December 11, 2024

Abstract: Currently, there is an increased demand for M50NiL steel from the aerospace, automotive, and nuclear industries to improve the characteristics of components, such as wear resistance, fatigue resistance, and surface hardness, while maintaining its corrosion resistance. Previous research has demonstrated that the nitride parameters are duration, temperature, and flow rate. The current investigation examines the efficacy of gas nitride on M50NiL steel from 500 to 550°C over 08–90 h according to the specific requirements of the specimens maintaining a gas ratio of 75:25 (NH_3:NH_3diss), a typical operational pressure within the range of 1–2 mbar, and an NH_3 flow rate of 0.4–0.5 l min^{-1}. Using a hydrogen chloride mixture as an activator for the steel surface, gas nitriding (GN) treatment is carried out in a partially dissociated ammonia atmosphere, resulting in the formation of the layers that are seen. In order to examine the phase transitions within the phase architecture and the chemical constituents of the gas-nitrided layer, methodologies such as energy-dispersive spectroscopy (EDS) and X-ray diffraction (XRD) were employed. The M50 NiL steel specimen, subjected to a thermal treatment at 550°C for a duration of 12 h, was found to possess an anomalously elevated concentration of nitrogen, according to the EDS evaluation. The results obtained from the XRD analysis of the gas nitrided layer indicated the existence of iron nitride phases, predominantly comprising α′-Fe, γ′-Fe4N, and α′N (nitrogen-enriched martensite). By micro-hardness assessment, it is apparent that at a temperature of 500°C over 24 h, the highest hardness value of 1,070 HV was achieved in the nitrided sample, which is approximately fourfold greater than that of the untreated specimen. In the case of case depth, it was observed that at 550°C for a duration of 24 h, the GN treatment resulted in a maximum case depth of 134 μm. The M50NiL specimen, designated GN 500, which underwent nitriding for 24 h, demonstrated the greatest wear resistance among the nitrided samples. Nitrided specimens are subjected to characterization along with electrochemical potentiodynamic corrosion assessment in an aerated 3.5% NaCl solution. The electrochemical evaluations indicated a substantial reduction in the corrosion current density of the specimen's post-nitriding, accompanied by a shift in the corrosion potential toward the noble direction with the extension of nitriding duration. The results of M50 NiL steel surface characteristics are enhanced after applying gas nitride coating. The findings indicate that controlled pressure GN effectively inhibits the precipitation of chromium nitrides, which is advantageous for the attainment of a thicker nitrided layer.

Keywords: gas nitriding, wear, corrosion, hardness, EDS

1 Introduction

Gas nitriding (GN) represents a case-hardening methodology wherein nitrogen is incorporated into the surface of a solid ferrous alloy by subjecting the metal to an appropriate temperature while in contact with nitrogenous gas, predominantly ammonia [1]. GN constitutes a category of low-temperature thermochemical treatment, with operational temperatures ranging from 400 to 590°C. During the nitriding procedure, the nitrogen introduced diffuses into the surface of the workpiece to a depth that is contingent upon both the duration and temperature of the treatment. This surface-hardening technique is frequently employed to enhance the wear resistance, hardness, and fatigue strength of metallic components. In contrast to plasma nitriding, which operates within a vacuum environment, GN occurs within a gaseous atmosphere typically consisting of ammonia (NH_3) and nitrogen (N_2) at elevated temperatures between 500 and 600°C [2]. Figure 1 shows the gas nitride furnace.

The process starts when the work components are placed within a retort or furnace that is hermetically

* **Corresponding author: C. Anil Kumar Reddy**, Department of Mechanical Engineering, Koneru Lakshmaiah Education Foundation, Vaddeswaram, 522502, India, e-mail: anilreddymechanical@gmail.com
Pothamsetty Kasi V. Rao, Boggarapu Nageswara Rao: Department of Mechanical Engineering, Koneru Lakshmaiah Education Foundation, Vaddeswaram, 522502, India
Begori Venkatesh: Mechanical Engineering, Vardhaman College of Engineering, Hyderabad, 501218, India

Figure 1: GN furnace.

sealed and contains a nitrogen-enriched gaseous atmosphere. To promote the diffusion of nitrogen into the metal's surface, the workpieces are heated until the desired nitriding temperature is reached. As nitrogen atoms penetrate the metal's lattice structure during the nitriding process, nitrides are created that greatly improve the surface properties. By adjusting several process variables, such as temperature, time, and gas composition, the amount of the nitrided layer can be controlled [3]. Depending on the required depth of the nitrided layer and the particular material being treated, the nitriding process typically takes several hours to several days [4].

To establish an optimized layer during GN, it is essential to utilize two-component atmospheres for the regulation of nitriding potential. The two gaseous components are ammonia and dissociated ammonia (NH_3 + NH_3diss. [75% hydrogen and 25% nitrogen]), along with ammonia and molecular nitrogen (NH_3 + N_2). By judiciously selecting the atmospheric composition and meticulously adjusting the flow rate of the atmosphere through the retort, it becomes feasible to generate layers with the desired phase composition (comprising $\varepsilon + \gamma' + \alpha$, $\gamma' + \alpha$, or α zones) at specified thicknesses for each zone. The dilution of ammonia with streams of dissociated ammonia (NH_3diss.) or nitrogen (N_2) yields a reduction in the nitriding potential, thereby facilitating enhanced control over the formation of the epsilon phase.

Upon the conclusion of the nitriding cycle, the workpieces undergo a methodical cooling process to ambient temperature, thereby reducing the likelihood of deformation or fracture. The GN technique presents numerous benefits, notably its capacity to achieve consistent nitriding depths across intricate geometries and an extensive variety of both ferrous and non-ferrous materials. The efficacy of the nitriding procedure is significantly contingent upon the precise regulation of GN parameters, specifically the concentrations of ammonia (NH_3) and nitrogen (N_2) in the gaseous medium utilized during the operation. Such regulation is paramount for ascertaining the integrity of the nitriding layer developed on the substrate surface. Conventional heat treatment techniques frequently prove inadequate in enhancing the surface characteristics of these shafts. They may fail to deliver adequate wear resistance or necessitate protracted processing durations, which can adversely influence production efficiency [5].

1.1 High-temperature bearing steel

Bearings are subjected to service temperatures surpassing approximately 150°C, and conventional low alloy steels are unable to retain the requisite surface hardness necessary to ensure an adequate fatigue life [6]. The limited corrosion resistance inherent in these steels renders them vulnerable to degradation due to environmental moisture, as well as to aggressive gaseous or liquid contaminants. Consequently, specialized steels are often utilized when these specific service conditions prevail [7]. Certain bearing steels are particularly well suited for applications at elevated temperatures. These steels are generally alloyed with carbide-stabilizing elements such as chromium, molybdenum, vanadium, and silicon, which serve to enhance their hot hardness and resistance to tempering [8]. The maximum operational temperatures (ranging from 315 to 350°C) correspond to conditions where the hardness at elevated temperature diminishes to a level below a minimum of 58–62 HRC (Rockwell C scale). An essential application of high-temperature bearing steels is found in aircraft and stationary turbine engines. For several years, M50 steel has been used to manufacture bearings that are incorporated into engine applications. The operational speeds of jet engines are being consistently elevated to enhance performance and efficiency; thus, the bearing steel utilized in these engines must possess enhanced section toughness to endure the stresses induced by increased centrifugal forces. Consequently, carburizing high-temperature bearing steels, such as M50-NiL and M50, are considerable [9]. The core toughness exhibited by these steels is more than double that of traditional through-hardening steels.

M50 NiL is a low carbon alloy steel with high nickel, which mainly serves as a type of high-temperature alloy steel for the spindle bearings of aero-engines due to its excellent properties of dimensional stability, high toughness, and contact fatigue resistance under high temperatures. Bearings sustain great pressure and friction during work; hence, the tribological performance of M50 NiL steel directly affects the normal running accuracy and reliable service life of the bearings, especially in a high-temperature environment [10].

M50NiL steel is a modified version of the standard AISI M50 bearing material. It has a reduced carbon content (from 0.85 to 0.13%) to improve fracture toughness and includes about 3.4% nickel. This nickel addition helps stabilize the austenite phase and prevents excessive formation of ferrite and retained austenite, which can negatively affect the material's properties. The steel is produced using vacuum induction melting and vacuum arc re-melting (VIM-VAR) processes. These methods ensure a cleaner steel with fewer inclusions, which is essential for enhancing fatigue life and overall performance in demanding applications. M50NiL exhibits excellent mechanical properties, including high fracture toughness and superior surface fatigue life. M50NiL is particularly advantageous in aerospace applications, where components are subjected to high stresses and temperatures. Its properties make it suitable for critical parts such as gears and rolling-element bearings in aircraft engines, where reliability and performance are essential. The material's ability to maintain performance under high Hertz stress (up to 4.83 GPa in rolling contact tests) and elevated temperatures (up to 589 K) enhances its suitability for high-speed aircraft and military applications, where operational reliability is crucial [11].

M50NiL is developed from standard AISI M50 by significantly reducing the carbon content from 0.85 to 0.13%. This reduction is aimed at improving fracture toughness, which is crucial for applications where material failure can occur due to fatigue spalls [12]. M50NiL includes an addition of 3.4% nickel. This nickel content helps stabilize the austenite phase and prevents the formation of excessive amounts of ferrite and retained austenite, which can negatively affect the material's performance [13]. The modifications in M50NiL, particularly the lower carbon content and the addition of nickel, enhance its fracture toughness compared to AISI M50 [9]. This improvement is essential for applications in advanced aircraft where materials are subjected to high stresses and potential fatigue [14].

The objective of this work is to use low-pressure GN, which has shown a considerable increase in surface hardness and resistance, to improve the surface attributes of M50 NiL steel. Prior studies have demonstrated that methods of surface hardening, including carburizing, can provide hardness values as high as 855 HV.

2 Materials and methods

2.1 Materials

A vacuum induction melting and casting furnace is employed for the synthesis of the experimental M50NiL steel, which subsequently undergoes forging and heat treatment. This alloy is also referred to as CBS-50NiL and AMS 6278 [15]. It finds application in high-temperature environments where the enhancement of surface strength and fatigue resistance is imperative. The molybdenum content in M50NiL confers exceptional wear resistance, while its low carbon composition facilitates remarkable toughness, making it a viable alternative to M50 for high-temperature applications (up to 316°C) in components such as bearings and gears. Furthermore, it possesses carburizing and nitriding capabilities, enhancing wear resistance and fatigue strength, while its core maintains substantial fracture toughness [16]. Figure 2 illustrates the compositional structure of M50NiL steel. In this investigation, M50NiL steel specimens measuring 10 mm × 10 mm × 5 mm were utilized. The samples are machined *via* electrical discharge machining (EDM) to attain dimensions of 10 mm × 10 mm × 5 mm each from a 25 mm diameter rod. Subsequently, the smooth surfaces of the samples are polished using silicon carbide waterproof emery sheets with grades

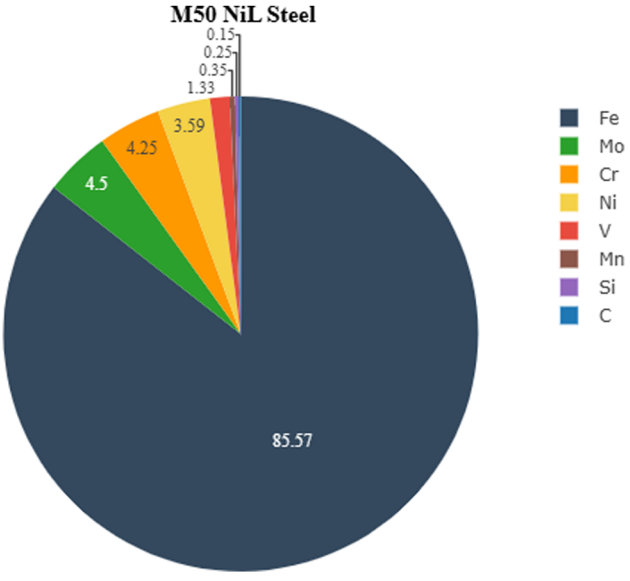

Figure 2: M50NiL steel composition (wt%).

1000 and 2000 [17]. Following the polishing process, the specimens are cleaned with acetone. The samples were categorized as GN500°C at 08, 12, 24 h; GN520°C at 08, 12, 24 h; 550°C at 08, 12, 24 h; GN510°C at 20, 30 h; and GN545°C at 90 h, culminating in 12 specimens designated for the nitriding treatment.

2.2 Gas nitriding

GN initiates with the meticulous preparation of samples, which are subjected to thorough cleaning and degreasing procedures to guarantee an immaculate surface. The GN furnace possesses dimensions of 750 mm in diameter and 1,800 mm in height, with a voltage capacity ranging from 220 V/400 V at 45 kW/72 kW. Ammonia (NH_3), exhibiting a purity level of 99.99%, was utilized as the nitriding atmosphere [18]. These specimens are then systematically placed in a sealed chamber. Figure 3 illustrates the schematic configuration of the GN procedure while sustaining a gas ratio of 75:25 (NH_3:NH_3 dissociated mix of hydrogen and nitrogen). It is suitable for the reaction $2NH_3$ + heat $2N + 3H_2$ and $2N + 3H_2 \rightarrow N_2 + 3H_2$, with a standard operational pressure maintained within the range of 0.2 MPa and an NH_3 flow rate of 0.4–0.5 l min^{-1}. The chamber is subsequently elevated to temperatures typically ranging between 500 and 550°C, at which point a nitrogen-rich gas, specifically ammonia (NH_3), is introduced. Nitrogen atoms from the gas permeate into the surface of the metallic specimens, thereby augmenting their properties. After a pre-established duration, usually extending from 8 to 90 h, the chamber is gradually cooled to avoid oxidation of the newly formed nitride layer. In this particular nitriding examination, samples were subjected to treatments at temperatures of 500, 520, and 550°C for 8, 12, and 24 h, as well as at 545°C for 90 h and at 510°C for 20 and 30 h, under meticulously controlled pressure conditions (100–200 kPa) and gas compositions (75–95% ammonia and 5–25% dissociated ammonia) [19]. Prior to the introduction of the nitriding gas, the samples were preheated in nitrogen to the processing temperature and subsequently cooled in nitrogen from the nitriding temperature to the ambient temperature. The nitriding gas constitutes a blend of ammonia and dissociated ammonia. The nitriding potential (K_n) is consistently monitored utilizing a hydrogen sensor and regulated by modulating the mixing ratios of ammonia to dissociated ammonia gas. A stable nitriding potential is upheld by continuously fine-tuning the flow rates of both ammonia and dissociated ammonia [20].

This procedure is meticulously crafted to augment the surface integrity of the rotating shafts, consequently enhancing their resistance to wear and their overall functionality. The GN methodology encompasses several pivotal stages, including the cleansing of surfaces, pre-oxidation treatment, plasma activation, and the regulated introduction of nitrogen and ammonia gases. These stages are intended to refine the treatment parameters to attain superior outcomes in comparison to the conventional techniques. By optimizing the heat treatment conditions, the innovative process not only fortifies surface strength but also reduces the duration of treatment, thereby augmenting manufacturing efficiency. This advancement holds particular significance within the automotive sector, where performance and dependability are of utmost importance. In the realm of specialized applications, GN treatments can be categorized into two distinct classes. The first is conducted under low gas pressure conditions (0.01 MPa), while the second is executed under normal atmospheric pressure conditions (0.1 MPa) for comparison. Ammonia was introduced into the furnace at a flow rate of 0.5 l min^{-1}. Subsequent to the GN process, all samples underwent a gradual cooling process to ambient temperature within an ammonia-enriched atmosphere [22].

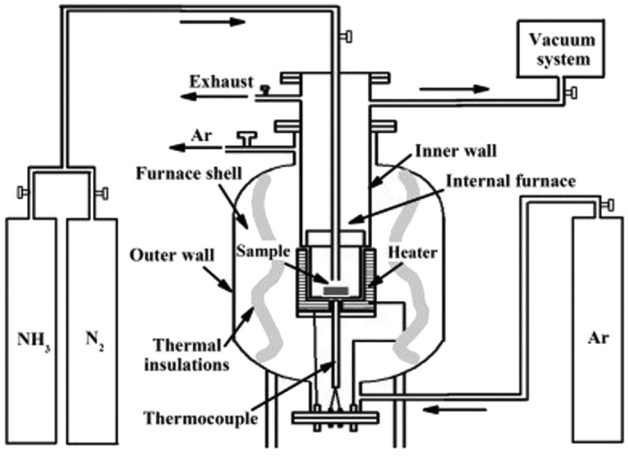

Figure 3: Detailed image of the GN process [21].

2.3 Characterization

Mechanical characterization of untreated and plasma-nitrided specimens is carried out to ascertain micro hardness; the Vickers hardness tester Economet VH 1MD is employed with a load of 100 g and a dwell time of 20 s. The case depth of the modified layer is examined utilizing an optical microscope, specifically the MET Scope-I, at magnifications of 100× and 500×. By employing AQUAREGIA for sample etching, the depth of the altered layer was quantified through optical microscopy. Scanning electron microscopy (SEM) combined with

energy-dispersive spectroscopy (EDS) was utilized to average measurements from two distinct locations on the sample using the Nova Nano SEM 450 apparatus, thereby analyzing the surface morphologies and elemental composition variations of the specimens [23]. Phase analysis of the nitrided samples was conducted using X-ray diffraction (XRD) techniques (BRUKER-D8 Advance) employing a Cu-Kα source with a wavelength of λ = 0.154093 nm, specifically for plasma-nitrided samples. The resultant diffraction patterns were obtained with a step size of 0.1° and a counting duration of 2 s per step within the 2θ range of 20–120°. A pin-on-disc tribometer (TE-165-SPOD and Magnum Engineers) is utilized to evaluate the wear performance of the specimens. The specimens, configured as discs, are rotated for 1,800 s at a velocity of 1,909 rpm, with a sliding distance of 3 mm (0.1 m/s), against a stationary M50 NiL sample measuring 10 mm × 10 mm. The standard contact load applied was 20 N. All tests were conducted in an open environment at an approximate temperature of 24°C. Electrochemical corrosion assessments were performed on plasma-nitrided M50 NiL samples using a Biologic-SP 300 Potentiostat apparatus, with durations of 2 h and 50 min and 30 min for open-circuit voltage (OCV) measurements, and a scan rate of 0.2 mV/s spanning from −1 V to +1 V.

3 Results and discussion

3.1 Phase structure after gas nitriding (XRD)

Using XRD (Bruker AXS, D8 Advance X-ray Diffraction system) with Cu-Kα radiation (λ = 0.15406 nm) in the angle range of 20–120° at an incidence angle of 0.1°, step size of 0.02°, and time per step of 2 s, the phase structures in the nitrided surfaces are examined.

Figure 4(a) presents the XRD patterns of the nitrided specimens subjected to treatment at GN500°C for 8, 12, and 24 h. The XRD analysis indicates that the nitrided layers predominantly comprise α-FeN, γ-Fe_3N, and Fe_3O_4, along with a minor proportion of γ-FeN for specimens treated at GN500°C. The principal phases generated during the nitriding process are the iron nitrides (α-FeN and γ-Fe_3N) with some iron oxide (Fe_3O_4). At the relatively lower treatment temperature of 500°C, a more significant quantity of α-FeN and Fe_3O_4 was detected. With the increase in treatment duration, the diffraction intensities of α-FN and γ-Fe_3N increased, whereas that of Fe_3O_4 decreased. The diffraction patterns reveal discernible variations in the peak intensities of γ-FeN and iron oxide (Fe_3O_4), underscoring the gradual development of these phases over time. The presence of γ-FeN diminishes after 8 h of nitriding as the nitride layers become increasingly prevalent. As the nitriding duration extends, the intensity of the γ-Fe_3N peaks tends to increase overall. The slight broadening of the peaks may suggest the presence of stress or strain within the layer as a consequence of the extended nitriding process. Over prolonged nitriding periods, the diffusivities of nitrogen and oxygen within the nitriding agent are augmented. Consequently, an increased quantity of nitrides and oxides, such as γ-Fe_3N and Fe_3O_4, is produced, resulting in a greater depth of the nitrided layer.

At a reduced treatment temperature of 520°C, a substantial quantity of Fe_3O_4 is detected in the GN520°C sample at the 08-h mark, as shown in Figure 4(b). As the duration of treatment is extended, the diffraction intensity associated with Fe_3O_4 exhibits a decline. This reduction can be attributed to the progressive emergence and development of alternative nitride phases, such as α-FeN, which increasingly assert dominance over time. The diffraction intensity of the α-FeN phase strengthens after a 12-h period of nitriding. This amplification in intensity is a consequence of the ongoing diffusion of nitrogen into the steel matrix, thereby facilitating the growth of α-FeN. GN at 520°C catalyzes the synthesis of iron nitrides, with the magnitude of nitride formation demonstrating a positive correlation with the duration of nitriding. XRD analysis reveals the presence of a pronounced α-FeN phase in the GN520°C specimen after 24 h. This observation signifies that the GN process conducted at 520°C for a duration of 24 h resulted in the emergence of a considerable quantity of the iron nitride phase, which is indicative of the nitrided layer. The existence of α-FeN implies effective nitrogen diffusion into the substrate, thereby enhancing the wear and corrosion resistance typically attributed to this phase. Evidently, the compound layer is primarily composed of γ-Fe_3N and γ-FeN along with α-FeN. The generation of these nitrides contributes to an improvement in surface hardness and wear resistance, as nitrides exhibit superior hardness and wear resistance compared to pure iron.

At an elevated treatment temperature of 550°C, as shown in Figure 4(c), a substantial quantity of α-FeN was detected in the GN550°C sample subjected to a 24-h duration. This phenomenon is likely attributable to the extended treatment period of 24 h, which facilitates extensive nitrogen diffusion into the steel matrix, culminating in the formation of a robust and enriched α-FeN phase. The sustained exposure at this high temperature permits adequate time for the nitrogen to infiltrate deeply, thereby resulting in a more pronounced evolution of this phase, which can markedly affect the mechanical properties and corrosion resistance of the material. As the duration of the nitriding treatment at 570°C was

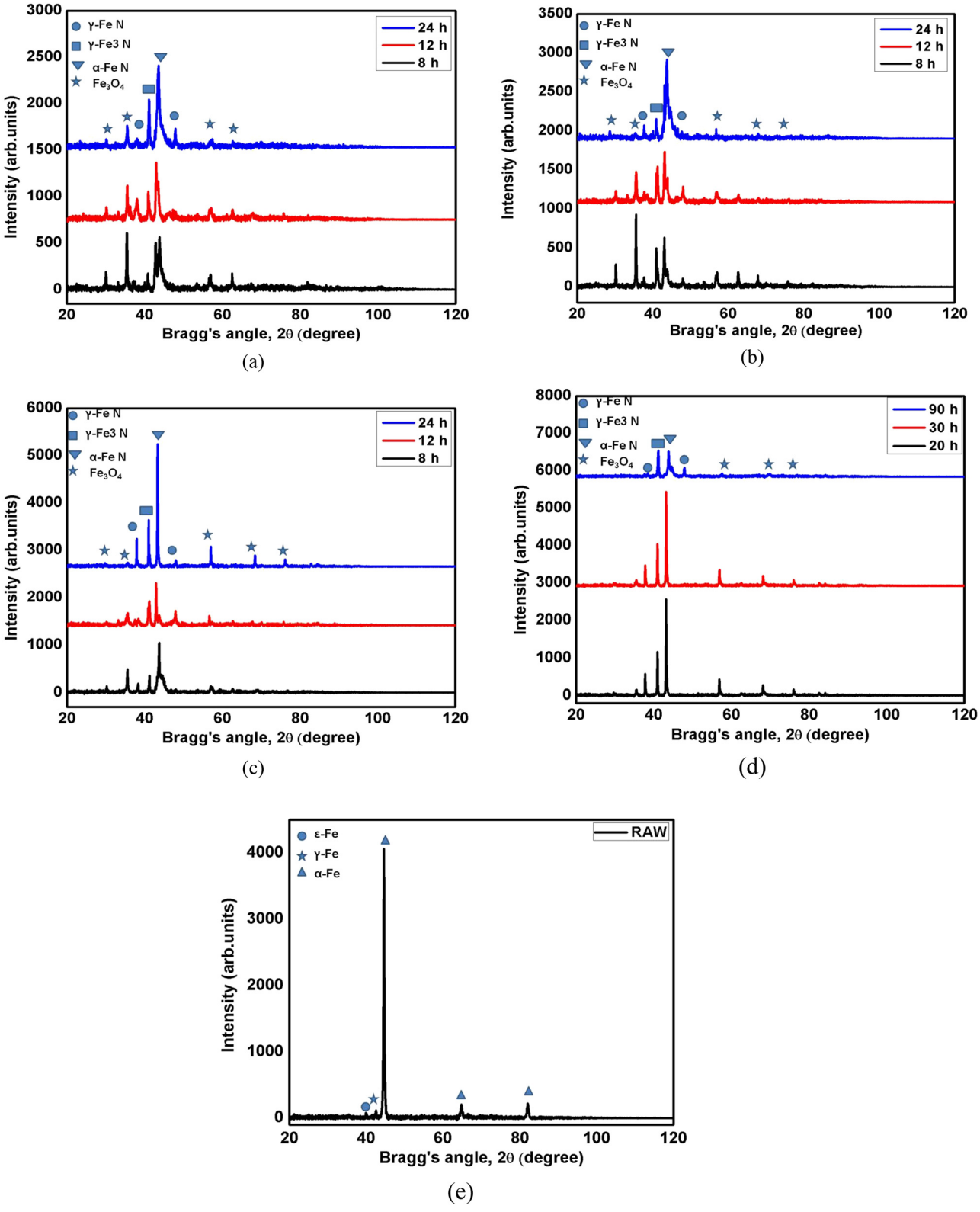

Figure 4: XRD profiles of the gas nitrided samples (500–550°C): XRD plots at (a) 500°C, (b) at 520°C, (c) at 550°C, (d) at 510°C for 20 and 30 h and 545°C at 90 h, and (e) for Raw M50 NiL.

incrementally prolonged, the diffraction intensity of the γ-FeN and γ-Fe_3N phases exhibited an increase in strength, peaking at 24 h. Furthermore, the concentration of Fe_3O_4 was significantly enhanced after a treatment duration of 12 h, coinciding with the formation of predominant nitride layers. Analysis of the diffraction patterns reveals discernible variations in the peak intensities of γ-FeN and iron oxide (Fe_3O_4), underscoring the progressive development of these phases over time. The intensity of the γ-FeN peaks generally increases with an increase in treatment duration. The marginal broadening of the peaks may suggest the presence of stress or strain within the layer as a consequence of extended nitriding.

Figure 4(d) illustrates the XRD patterns corresponding to the nitrided specimens at temperatures of 510 and 545°C. XRD analysis elucidated that the nitrided layers primarily comprise α-FeN and γ-Fe_3N, in addition to minor quantities of γ-FeN and Fe_3O_4 present in the specimens. The XRD patterns signify the existence of γ-FeN and γ-Fe_3N, along with a limited amount of γ-FeN and Fe_3O_4 identified in the GN545°C specimen at 90 h. The emergence of these nitride phases contributes to an enhancement in surface hardness and wear resistance, attributable to the superior hardness and wear-resistance properties of nitrides compared to pure iron. The variations in the phase composition with respect to nitriding duration underscore the dynamic characteristics of the nitriding process, which exerts an influence on the microstructure and mechanical attributes of the treated material.

Figure 4(e) illustrates the XRD patterns corresponding to both untreated and nitrided M50NiL samples. The phase composition of the nitriding layers on M50NiL steel is contingent upon the nitriding temperature, the duration of the process, and the nitrogen potential. As represented in the figure, the phases observed in the untreated sample are predominantly comprised of α-Fe (ferrite) phase, along with a lower quantity of ε-Fe and γ-Fe (austenite phase). Conversely, the nitriding process facilitates the emergence of new phases that evolve in accordance with the nitriding temperature.

Following GN at 510°C, the XRD examination of the specimen GN510°C at 30 h indicates the substantial formation of α-FeN and γ-Fe_3N, along with a minimal amount of Fe_3O_4 and γ-FeN phases. The γ-FeN phase emerges as the dominant phase detected across the samples, substantiating the development of a nitride layer during the nitriding process. The intensity of the α-Fe peak, representative of the ferrite phase, demonstrates an increasing trend as the duration of nitriding diminishes, suggesting that nitrogen diffusion becomes less efficient with reduced nitriding times.

Analysis of the diffraction patterns reveals significant disparities in the peak intensities of γ-FeN and iron oxide (Fe_3O_4), particularly at elevated temperatures such as 550°C and extended durations. These alterations underscore the progressive formation and expansion of these phases over temporal intervals. The augmentation of the γ-FeN phase implies enhanced nitrogen diffusion, while the more prominent Fe_3O_4 peaks suggest that oxidation is increasingly pertinent at this elevated temperature and prolonged duration, potentially influencing the protective attributes of the nitrided layer.

3.2 EDS analysis of gas-nitrided samples

EDS was performed utilizing an FEI NOVA 450 apparatus integrated with a scanning electron microscope (SEM), facilitating an in-depth analysis of the chemical composition of the specimen. The nitrided M50NiL samples are subjected to EDS analysis aimed at elucidating their chemical composition, with particular emphasis on the nitrogen content.

EDS measurements were systematically executed at arbitrary locations across the nitrided surface. The data generated from EDS analysis are presented in the format of spectra, with peaks corresponding to the elemental constituents of the sample under investigation. The EDS findings pertaining to the gas-nitrided layer of the M50NiL specimens are illustrated in Figure 5(a)–(g).

From Figure 5(a) and Table 1, the weight percentage of components identified in the EDS spectroscopy analysis for the untreated M50NiL specimen is quantified as 9.9% carbon, 0.1% aluminum, 0.2% silicon, 0.1% titanium, 1.1% vanadium, 3.6% chromium, 0.3% manganese, 76.4% iron, 0.9% cobalt, 2.8% nickel, 0.1% copper, 4.2% molybdenum, and 0.4% tungsten.

From Figure 5(b), the EDS analysis conducted at 500°C demonstrated that the GN500°C sample subjected to 12 h exhibited an elevated surface nitrogen concentration of 6.7 wt%, whereas the GN500°C sample exposed for 8 h presented a significantly lower nitrogen content of 0.2 wt%. The augmented nitrogen concentration observed in the GN500°C sample at 12 h is representative of a more efficient nitrogen diffusion into the surface layer, which is pivotal for the enhancement of surface hardness and wear resistance. The observed increase in nitrogen content can be attributed to the favorable nitriding conditions that allow for the establishment of a stable nitride layer due to the synergistic effects of elevated temperature and prolonged duration. Furthermore, the carbon content increases to 12.9 wt% in comparison to the untreated sample, which

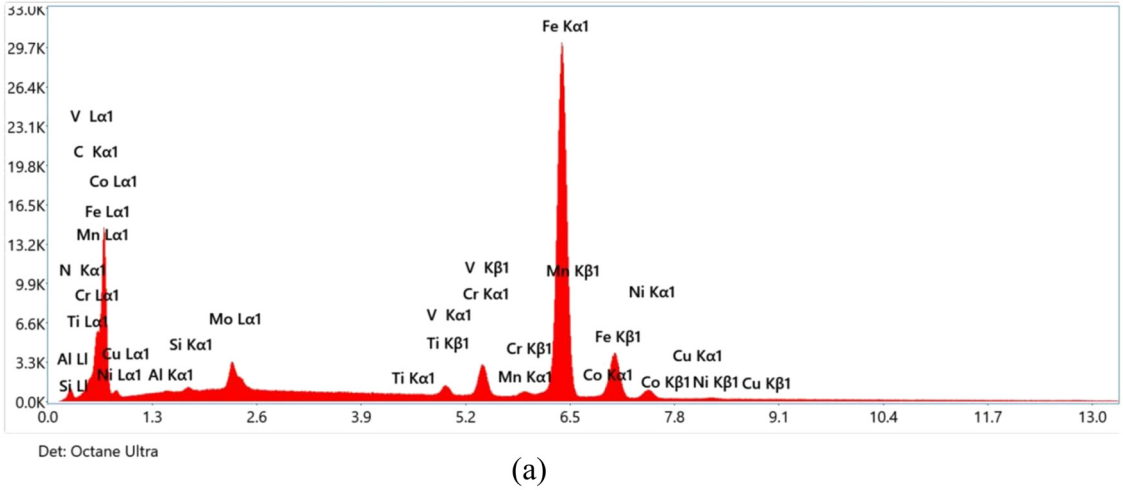

(a)

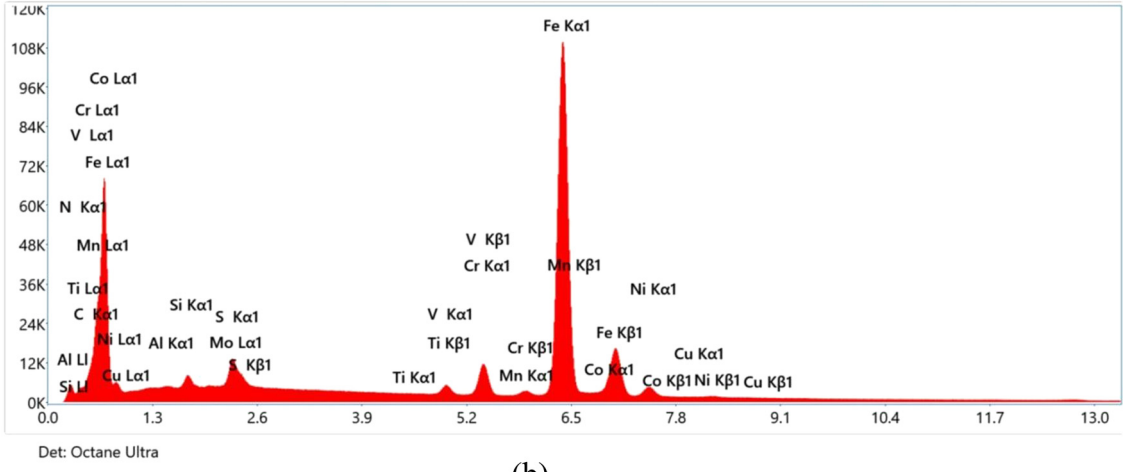

(b)

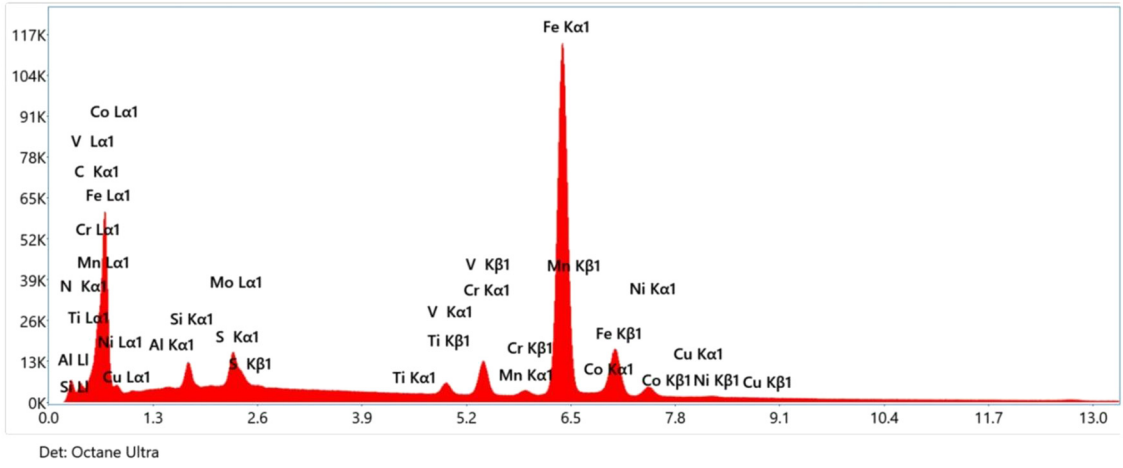

(c)

Figure 5: EDS analysis of gas-nitrided M50NiL specimens. EDS profile of (a) the untreated sample, (b) GN500°C at 12 h, (c) GN520°C at 12 h, (d) GN550°C at 12 h, (e) GN545°C at 90 h, (f) GN510°C at 30 h, and (g) GN500°C at 08 h.

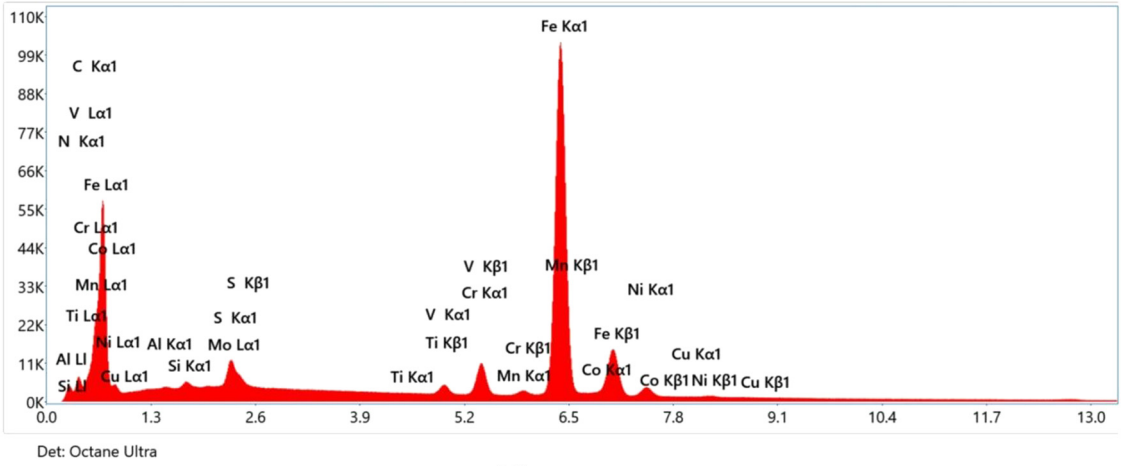

(d)

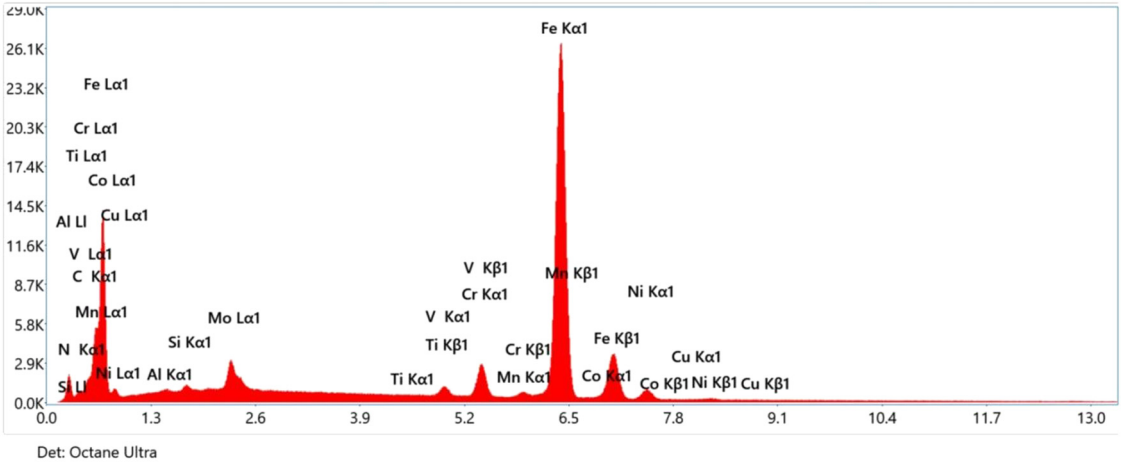

(e)

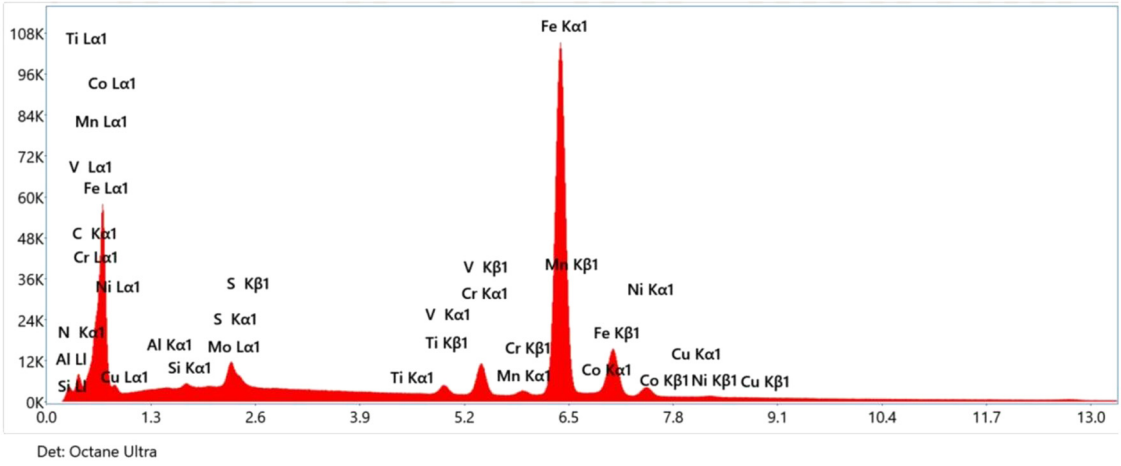

(f)

Figure 5: (*Continued*)

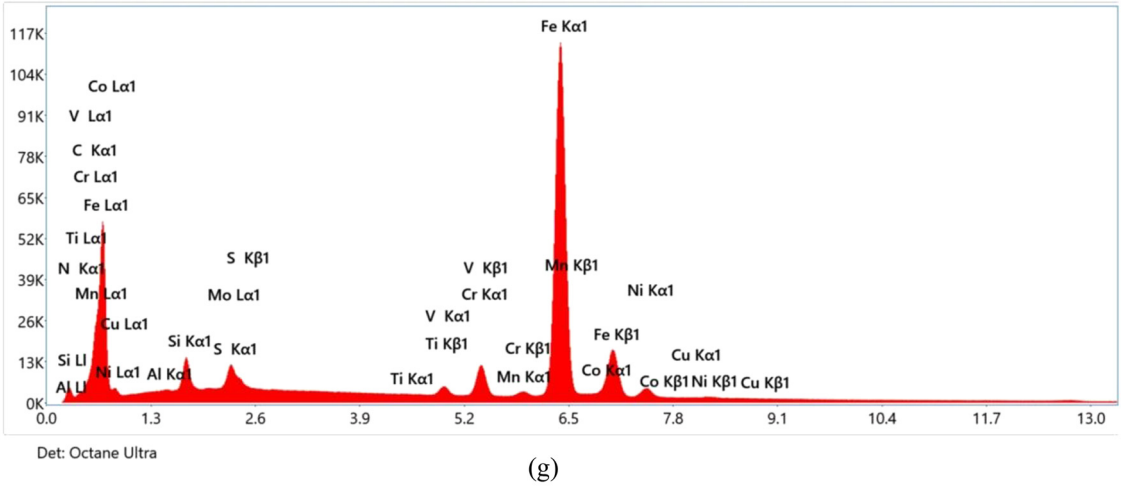

(g)

Figure 5: (*Continued*)

contributes positively to the mechanical properties. The reduction in iron content to 65.6 wt% signifies nitrogen absorption, a typical phenomenon prevalent during nitriding processes. This transformation entails the conversion of iron atoms into iron nitrides, which act as hard and wear-resistant precipitates within the steel matrix.

As shown in Figure 5(c), at 520°C, the nitrogen content is recorded at a minimum of 0.5 wt% for the GN520°C sample at 8 h, while the maximum nitrogen content reached 10.6 wt% for the GN520°C sample at 12 h, which concurrently exhibited a high carbon content of 15.4 wt%. The disparity in nitrogen content observed between these two samples can be ascribed to the variations in nitriding duration. This comparatively low nitrogen content implies that the nitriding process conducted during this specific duration (8 h) may have been inadequate to realize optimal nitrogen diffusion into the surface layer, resulting in a less pronounced hardening effect. Conversely, the prolonged nitriding duration of 12 h for the GN520°C sample allows for a more significant diffusion of nitrogen atoms into the steel, thereby considerably enhancing the nitrogen content.

EDS identified a diminished nitrogen concentration of 8.6 wt% for the GN550°C at 08 h specimen in comparison to other samples subjected to nitriding at 550°C with reference to Figure 5(d). This reduced nitrogen concentration can be ascribed to the shortened nitriding duration of 8 h, which imposes constraints on the temporal availability for nitrogen atoms to penetrate deeply into the steel substrate, culminating in a diminished nitrogen concentration within the nitrided layer. Conversely, the 550°C sample at 12 , exhibiting a nitrogen concentration of 14.6 wt%, demonstrates a superior surface nitrogen concentration. The protracted

Table 1: EDS analysis of gas-nitrided M50NiL by SEM

Element (wt%)	Untreated	GN500°C at 12 h	GN520°C at 12 h	GN550°C at 12 h	GN545°C at 90 h	GN510°C at 30 h
Carbon (C)	9.9	12.9	15.4	10.2	11.3	9.0
Nitrogen (N)	0.0	6.7	10.6	14.6	3.0	15.7
Aluminum (Al)	0.1	0.6	0.2	0.3	0.3	0.3
Silicon (Si)	0.2	0.9	1.4	0.4	0.2	0.2
Sulfur (S)	0.0	0.0	0.0	0.0	0.0	0.0
Titanium (Ti)	0.1	0.0	0.0	0.0	0.0	0.0
Vanadium (V)	1.1	0.7	0.9	0.7	0.8	0.7
Chromium (Cr)	3.6	2.9	2.9	2.8	3.1	2.8
Manganese (Mn)	0.3	0.1	0.1	0.1	0.1	0.1
Iron (Fe)	76.4	65.6	59.2	62.4	71.9	63.9
Cobalt (Co)	0.9	2.1	2.0	1.8	2.1	1.8
Nickel (Ni)	2.8	3.2	2.9	2.8	3.2	2.9
Copper (Cu)	0.1	0.6	0.5	0.5	0.6	0.5
Molybdenum (Mo)	4.2	3.7	4.0	3.3	3.3	3.0

nitriding duration of 12 h facilitates more comprehensive nitrogen diffusion into the steel, resulting in a markedly elevated nitrogen concentration. This augmented nitrogen concentration is instrumental in fostering the development of a thicker and more resilient nitrided layer, thereby enhancing surface hardness and wear resistance.

As shown in Figure 5(f), at 510°C, the GN510°C specimen at 20 h, exposed to an extended nitriding duration of 20 h, reveals a reduced nitrogen concentration (6.3 wt%) and a carbon concentration of 8.7 wt%, whereas the 30-h nitrided sample (GN510°C at 30 h) displays an elevated nitrogen concentration of 15.7 wt%, in conjunction with a carbon concentration of 9.0 wt% and an iron concentration of 63.9 wt%, which is lower than that of the untreated sample (76.4 wt%). This observation signifies a more efficacious and prolonged nitrogen diffusion, culminating in a heightened surface nitrogen concentration. The extended nitriding duration permits a more substantial synthesis of nitrides, which augments surface hardness and wear resistance. The amalgamation of increased nitrogen and carbon concentrations facilitates the formation of a sophisticated microstructure comprising nitrides and carbonitrides. The nitrogen content in the nitrided sample GN545°C at 90 h is 3.0 wt%, accompanied by 11.3 wt% carbon and 71.9 wt% iron, when subjected to treatment at 545°C, as shown in Figure 5(e). The relatively moderate nitrogen concentration is a consequence of the specific parameters governing the GN process at this temperature and duration. At 545°C, the nitriding process is meticulously optimized to ensure adequate nitrogen diffusion into the steel, engendering stable nitrides such as γ-Fe_3N and α-FeN. Nevertheless, the temperature is judiciously regulated to preclude excessive nitrogen absorption, which may precipitate brittleness.

The findings derived from the EDS analysis demonstrate a clear correlation between the nitrogen content in the steel and the duration of the solution nitriding process, notwithstanding that the EDS measurements were conducted at arbitrary locations on the steel surface. The minimum nitrogen content recorded is 0.2 wt% for the GN500°C sample at 08-h, as shown in Figure 5(g), whereas the maximum is 15.7 wt% for the GN510°C sample at 30 h. This observation suggests that, in general, at lower temperatures, an extended nitriding duration facilitates enhanced diffusion of nitrogen into the steel matrix. In contrast, at elevated temperatures, short nitriding duration suffices for adequate nitrogen absorption. This extensive range underscores the significant influence of nitriding parameters, specifically temperature, and duration, on the incorporation of nitrogen into the steel structure. From the above work, it is evident that the gas nitride sample microstructure has a compound layer up to 4 µm, which enhances wear resistance.

3.3 Surface mechanical properties (hardness, corrosion, and wear)

3.3.1 Micro hardness

A Vickers microhardness testing apparatus (ECONOMET VH 1MD) is employed to quantify the microhardness profiles of the nitrided layers for 10 s under the application of a 100 g load. To guarantee the precision of the measurements, the average value of three indentations made at an identical depth within the nitrided layer was utilized.

The microhardness profile of the nitrided specimens, characterized by nitriding temperatures and durations ranging from 500 to 550°C and 8 to 90 h, respectively, is illustrated in Figure 6. The surface microhardness of the nitrided M50NiL steel exceeds 950 HV, thereby indicating that GN can markedly enhance surface microhardness. The hardness of the untreated M50NiL specimen is approximately 297 HV. The surface hardness of the samples exhibited variation in response to alterations in nitriding temperatures and soaking times, while the resultant hardness was found to be within the range of 950–1,070 HV.

The hardness profile reveals a peak hardness of roughly 1070.5 HV at 500°C for a duration of 24 h, likely attributable to the optimal interplay between temperature and nitriding duration, which fosters the development of a high-hardness compound layer and fine nitride precipitates while concurrently minimizing the potential for grain coarsening or excessive nitrogen diffusion that could otherwise compromise surface hardness. The recorded surface hardness values attained 1070.5 HV, which is approximately fourfold that of the untreated nitrided material. This extraordinary enhancement in surface hardness can be ascribed to two

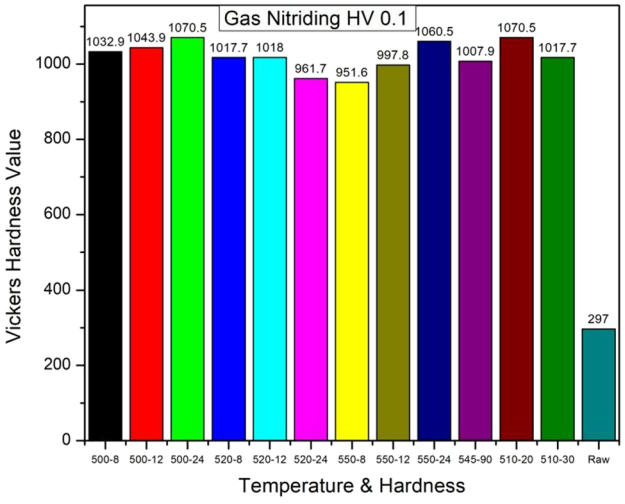

Figure 6: Hardness profile for GN specimens.

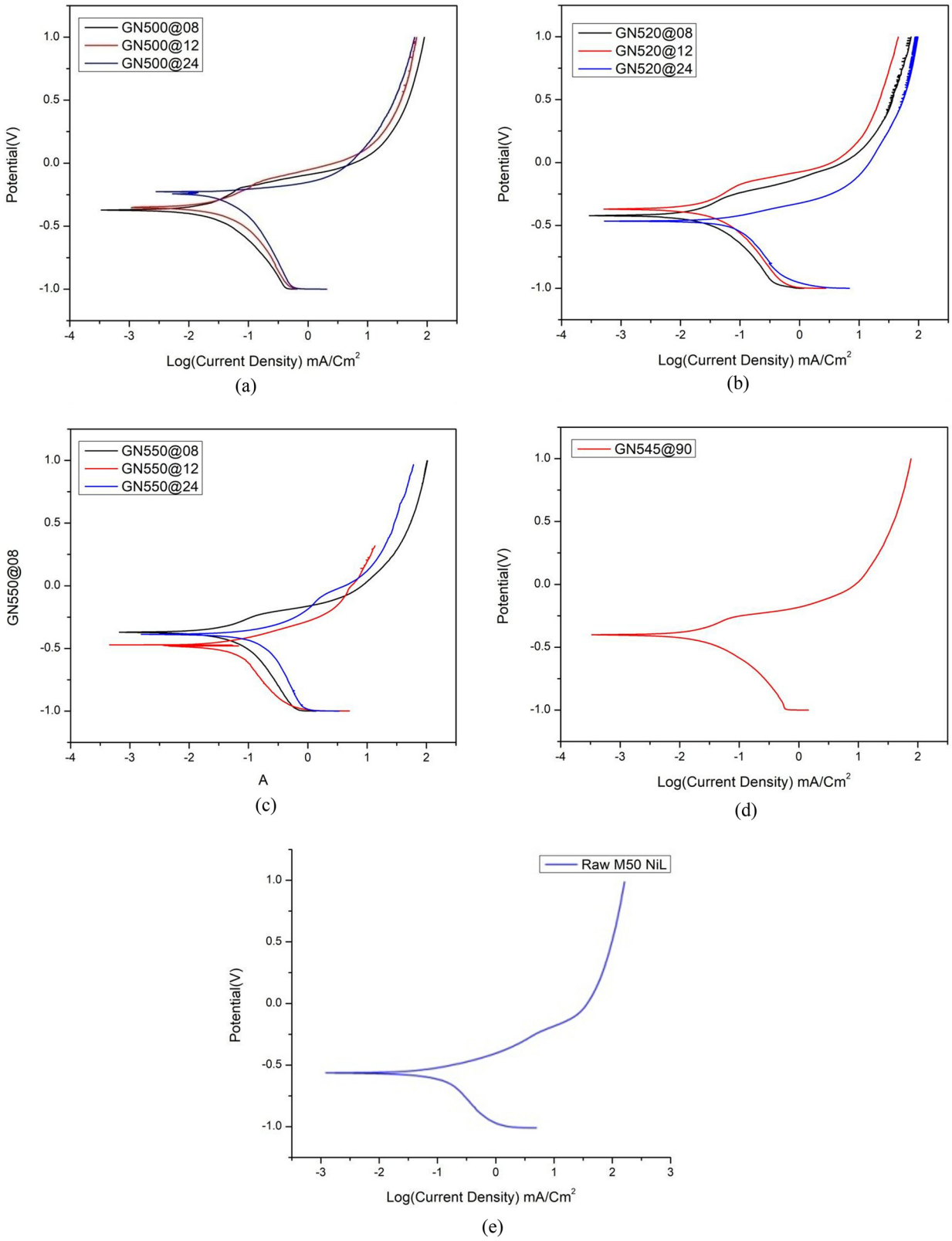

Figure 7: Tafel plots (Tp) of gas-nitrided samples at 500, 520, 550, 545°C and Raw for 8, 12, 24, and 90 h, respectively. Tp at (a) 500°C, (b) at 520°C, (c) at 550°C, (d) at 545°C, and (e) for the Raw sample.

principal factors: the emergence of a high-hardness compound layer and the considerable lattice distortion induced by the diffusion of nitrogen atoms.

Upon nitriding at 520°C, a peak hardness of approximately 1,018 HV is noted after 12 h, potentially due to the generation of a dense and fine-grained nitride layer, which augments the surface hardness of the material by conferring increased resistance to deformation. At 550°C, the specimen GN550°C subjected to 24 h of nitriding displays a maximum hardness of approximately 1,060 HV, reflecting the efficacious hardening achieved under these conditions. The elevated hardness is predominantly linked to the formation of hard nitrides, which enhance the surface hardness of the steel. Nonetheless, while the hardness is significantly increased, it is crucial to acknowledge that this temperature may also facilitate the formation of excess nitrogen compounds, which could contribute to brittleness. Despite this consideration, the substantial hardness of the nitrided layer signifies a successful hardening process within the delineated parameters, such as GN550°C.

At a temperature of 510°C, the peak hardness reaches approximately 1,070 HV following a nitriding duration of 20 h, subsequently diminishing to approximately 1,017 HV after 30 h. This observed reduction in surface hardness is presumably attributable to the deeper diffusion of nitrogen within the substrate, resulting in a nitride layer that is thicker yet less concentrated, ultimately leading to a decline in surface hardness. Precipitates of a specific size are deemed most effective in impeding the movement of dislocations, thereby facilitating maximal strengthening and hardening. With extended nitriding durations, the precipitate particles tend to increase in size and exhibit a greater susceptibility to coarsening, culminating in a reduced precipitate density and, consequently diminished hardness.

At a nitriding temperature of 545°C, the specimen subjected to nitriding for 90 h demonstrates a maximum hardness of approximately 1,007 HV, primarily attributable to the prolonged duration coupled with the favorable nitriding temperature. The extended duration of nitriding permits a more profound and uniform diffusion of nitrogen into the steel matrix, engendering the formation of robust nitrides and a well-developed nitrided layer. At this increased temperature, the generation of stable and hard phases, such as γ′-Fe_3N and γ-Fe_4N, is promoted, significantly enhancing the surface hardness. Furthermore, the meticulously controlled nitrogen levels throughout this nitriding process guarantee a high density of hard nitrides while preventing the onset of excessive brittleness, thereby augmenting the overall hardness and wear resistance of the material.

The findings indicate that when the nitriding temperature surpasses 500°C, particularly at 550°C, the micro hardness of the specimen GN550°C at 8 h is recorded at 951 HV0.1, which is comparatively lower than that of the other samples. This observed decrease in hardness is likely a consequence of the diminished density of the ferrite phase as the heat treatment temperature increases. Specimen GN500°C at 24 h exhibits a superior micro hardness profile in the surface layer relative to the other specimens. The maximum thickness of the nitride layer, measuring 210.00 µm, is observed in the sample nitrided at 510°C for 20 h. The surface hardness is contingent upon the duration of nitriding, given a constant temperature; however, the associated case depths of the nitrided samples tend to increase with increasing temperatures.

The examination of the GN data unveils several compelling insights. Although extended nitriding duration frequently results in enhanced surface hardness, the relationship is not uniformly linear. Certain specimens demonstrate a reduction in hardness following prolonged treatment, indicating a multifaceted interaction among variables such as nitrogen diffusion and nitride coarsening. Furthermore, temperature significantly influences this process. Elevated temperatures may hasten nitride coarsening, potentially resulting in a decrease in hardness over extended durations. Consequently, meticulous selection of nitriding parameters, especially temperature and time, is vital for attaining the desired surface hardness profile while circumventing adverse effects on the material. Prior researchers have also indicated that the hardness values of both the compound and diffusion layers are substantially affected by the nitride layer formed at varying temperatures during the nitriding process. Enhanced surface hardness has been associated with improved corrosion resistance. In addition to augmenting surface hardness, the compound layer has been identified as a key contributor to the exceptional wear and corrosion resistance of nitrided components [23].

3.3.2 Corrosion behavior

Potentiodynamic anodic and cathodic polarization curves are produced by electrochemical testing in a 3.5% wt. NaCl electrolyte solution using a Biologic SP300 potentiostat that is operated at a scan rate of 0.5 mV/s under the supervision of EC Lab software.

Figure 7(e) illustrates potentiodynamic polarization curves for both untreated M50NiL steel and gas-nitrided specimens. Through the analysis of the Tafel plots, the corrosion parameters E_{corr}, I_{corr}, and the corrosion rate were derived and are presented in Figure 8. It is evident that the corrosion potential of the nitrided specimen shifts toward the anodic region. This shift suggests a reduction in the thermodynamic tendency for the corrosion reaction

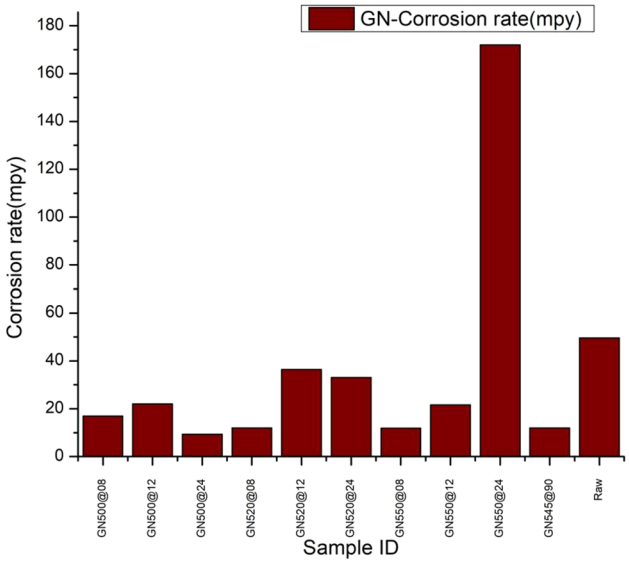

Figure 8: Corrosion rate for gas-nitrided samples and untreated.

within the system. In comparison to the untreated steel, the corrosion potential (E_{corr}) of the nitrided specimens is displaced toward a more noble potential, indicating a diminished susceptibility to corrosion. The potential range for the cathodic branch of both untreated and nitrided materials spans from −0.5 to −1.0 V, with the open-circuit potential situated approximately between −0.2 and −0.5 V. Furthermore, the cathodic branch of the presented curves correlates with the oxygen reduction reaction. Both untreated and nitrided specimens exhibit cathodic passivation characteristics. The curve corresponding to the untreated sample reveals a brief passive region, indicating that M50NiL steel is prone to corrosion in NaCl solution. Conversely, all nitrided specimens demonstrate prolonged passive regions and more positive corrosion potentials, signifying that nitriding at various temperatures enhances corrosion resistance. This improvement is attributed to the development of dense nitride compound layers on the surface. Consequently, nitrided specimens exhibit heightened resistance to anodic dissolution, as evidenced by their reduced polarization current density at equivalent anode electrode potentials compared to the untreated sample. The corrosion current density (I_{corr}) and corrosion rate for nitrided steel are markedly lower than those for untreated steel. Specifically, the untreated specimen displays an I_{corr} of 108.2 µA, whereas nitrided specimens reveal substantially lower values. This observation indicates that nitrided samples possess superior corrosion resistance relative to their untreated counterparts.

The corrosion data presented in Figure 7(a) indicate that the GN500°C sample subjected to a 24-h nitriding process exhibits an extended passive region, increased polarization resistance, and diminished corrosion current density, thereby signifying enhanced corrosion resistance. This superior performance is likely attributable to the nitriding treatment at 500°C for a duration of 24 h, which yields a more uniform and stable nitrided layer, effectively augmenting the specimen's resistance to corrosion in contrast to samples subjected to lower temperatures for shorter durations, wherein the nitrided layer may exhibit less development and inadequate protective qualities. When subjected to nitriding at 500°C for 24 h, the specimen demonstrated a corrosion rate of 9.3816 mpy, which is substantially lower than the corrosion rate of the untreated sample, recorded at 49.5 mpy. Among the nitrided specimens, the GN500°C at 24 h sample displayed the most favorable corrosion performance, characterized by a corrosion current (I_{corr}) of 20.479 µA, which is significantly lower than that of the other samples. This enhanced performance in terms of corrosion resistance can be partly ascribed to the specimen's markedly elevated microhardness, as a harder surface typically confers increased resistance to both corrosion and wear. Furthermore, the GN500°C at 24 h sample exhibited a more positive zero current (E_{corr}) of −231.8 mV, in contrast to the untreated material, which recorded −553.9 mV. Additionally, the OCV measurements of −0.24 further substantiates that the nitrided steel GN500°C at 24 h possesses a less noble corrosion potential, thereby accentuating its superior corrosion resistance.

As shown in Figures 8 and 7(b), the GN520°C at 08 h sample demonstrates a corrosion rate of 12.02 mpy, which is deemed optimal for GN at 520°C owing to the establishment of a well-balanced nitrided layer. This specific temperature and duration likely facilitate the formation of a stable and adequately thick protective layer that effectively enhances corrosion resistance without engendering brittleness or compromising the integrity of the layer. In comparison to other nitrided samples treated at 520°C, the GN520°C at 12 h sample exhibits markedly accelerated anodic kinetics, as evidenced by its elevated corrosion current density (I_{corr}). Conversely, localized regions exhibiting compromised passivity may be experiencing rapid deterioration, culminating in the high overall corrosion rate of 36.4 mpy, which indicates an increased susceptibility to corrosion attributed to diminished protection against corrosive agents. Figure 7(c) suggests the presence of a substantial passive range for the GN550°C at 08 h sample, likely resulting from the development of a thicker nitride layer. This augmented layer serves as an effective protective barrier, resulting in a reduced corrosion rate of 11.8 mpy, which signifies robust resistance, particularly under conditions of elevated temperature and moderate duration.

From Figure 7(d), GN545°C at 90 h demonstrates a corrosion rate of 11.9 mpy, highlighting its superior resistance even when subjected to elevated temperatures and extended

exposure durations. This remarkable performance is attributed to the development of a robust and well-formed nitrided layer at 545°C for 90 h, which offers effective defense against corrosion. Furthermore, its corrosion potential (E_{corr}) of −402.2 mV is relatively more positive in comparison to untreated steel, indicating a greater potential necessary to trigger corrosion reactions. This phenomenon effectively postpones the initiation of corrosion to less negative potentials, thereby rendering the nitrided steel less vulnerable to corrosive processes. Additionally, the OCV measurements of −0.42 V suggest a less noble corrosion potential, indicating that the nitrided layer possesses strong adhesion and enhanced stability, thereby augmenting the overall corrosion resistance of the steel.

The GN procedure generally improves corrosion resistance by creating a hard, protective, nitrogen-enriched layer on the steel surface. Nevertheless, for the sample GN550°C at 24 h, nitriding at 550°C for 24 h results in markedly elevated anodic kinetics, with a corrosion current density (I_{corr}) of 375.4 µA as shown in Figure 7(c), culminating in the highest corrosion rate within the group. This reduction in efficacy may be ascribed to excessive nitrogen diffusion at this temperature and duration, which could lead to the brittleness of the nitrided layer and susceptibility to cracking, thereby diminishing its protective efficacy. The results indicate that lower temperature nitriding significantly enhances corrosion resistance, with the samples treated at 500°C exhibiting the most favorable corrosion behavior. Nitrided samples display superior corrosion resistance in comparison to untreated samples, with the exception of the sample nitrided at 550°C for 24 h, which demonstrates diminished corrosion resistance attributable to the aging factor.

3.4 Tribological performance (Wear and COF)

The experimental setup for the pin-on-disc wear apparatus is depicted in Figure 9, wherein the tests are conducted under a constant load of 20 N and a sliding velocity of 1.0 m/s while maintaining a consistent sliding distance of 3,600 m, thereby controlling all other parameters. The above parameters are selected for high-temperature bearings, and other parameters can be achieved through optimization models. The results pertaining to the coefficient of friction (COF) are illustrated in Figure 10(a)–(d), whereas the wear rate is represented in Figure 10(e).

Figure 10(a)–(e) illustrates the friction coefficients and wear rates of both untreated and nitrided M50NiL steel

Figure 9: Pin on the disc apparatus.

specimens subjected to testing against a tungsten carbide (WC) ball for a duration of 3,600 s under a load of 20 N. The nitrided specimens demonstrate relatively uniform friction coefficients attributable to the elevated hardness of the nitrides present on the modified surface. The untreated specimen exhibits a friction coefficient of 0.5773, which surpasses those recorded for the nitrided specimens. This observation signifies that the development of a nitrided layer not only augments surface hardness but also enhances tribological properties. As depicted in Figure 10(d), the GN545°C specimen at 90 h reveals a friction coefficient of 0.1154, which is lower in comparison to the other specimens evaluated. In juxtaposition with the untreated specimen, the friction coefficients of the nitrided specimens are diminished during the initial phase, subsequently increasing to stabilized conditions. During the stable phase, the friction coefficients of the nitrided samples processed at 500°C for 24 h, 510°C for 30 h, 520°C for 12 h, and 550°C for 24 h (*i.e.*, from 500 to 550°C) are approximately 0.2900, 0.3418, 0.2978, and 0.3054, respectively. The friction coefficient of the nitrided samples exhibits an increasing trend in relation to both treatment duration and temperatures. The GN510°C at 20-h sample displays a comparatively elevated friction coefficient of 0.3424 under a load of 20 N. To further elucidate the wear characteristics of the untreated and plasma-nitrided specimens, the results are presented in Figure 10(e).

As shown in Figure 10(a), the GN500°C at 24-h specimen exhibits the lowest wear rate of 0.16×10^{-6} g/m (−0.34609 µm) along with a friction coefficient of 0.2900,

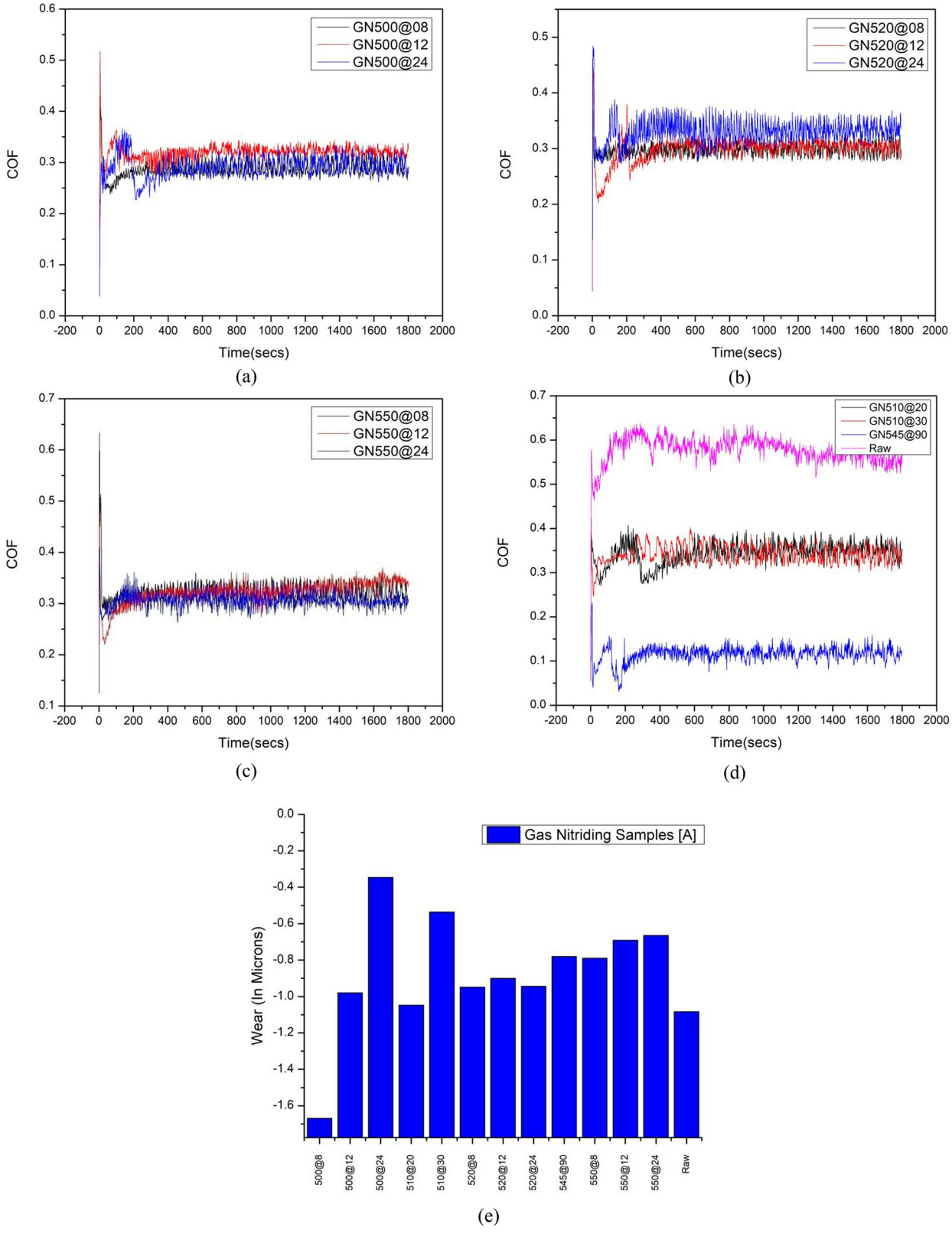

Figure 10: COF of the specimens treated at different durations for different nitriding temperatures: (a) 500°C, (b) 520°C, (c) 550°C, (d) 510°C, and 545°C, and (e) wear rates (WR) of untreated and gas nitrided samples for 500°C to 550°C.

which is remarkably low for a specimen subjected to nitriding at 500°C. Furthermore, this specimen exhibits superior hardness and corrosion resistance when compared to the other specimens evaluated, thereby demonstrating its efficacy in enhancing both wear and corrosion characteristics. In contrast, the untreated specimen presents a substantially elevated wear rate of 0.52×10^{-6} g/m (−1.08422 μm). Among the specimens that underwent nitriding at 500°C, the one characterized by the most significant wear resistance is the GN500°C at 24-h specimen, as evidenced by its minimal wear rate value. The surface microstructures of the GN500°C at 24-h specimen indicate that the formation of the α-FeN phase during nitriding at 500°C is advantageous for augmenting wear resistance. The GN500°C at 08-h specimen displays a considerably high wear rate of 0.83×10^{-6} g/m, surpassing that of the untreated specimen (−1.66915 μm). This elevated wear rate may be ascribed to an inadequate nitriding duration, which likely resulted in a thinner and less protective nitride layer. This observation implies that, notwithstanding the nitriding procedure, the wear resistance at this specific temperature and duration is relatively ineffective, potentially owing to insufficient nitrogen diffusion or a less stable nitrided layer. Additionally, this specimen exhibits a friction coefficient of 0.2867, signifying diminished resistance to wear in comparison to the other nitrided specimens.

As shown in Figure 10(b), the GN520°C at 12-h specimen has exhibited a low wear rate of 0.41×10^{-6} g/m (−0.90077 μm), which is lower than that of other specimens treated at 520°C. The wear resistance of the 520°C specimen at 12-h is notably superior to that of the samples nitrided at 520°C, with a value of 0.370×10^{-3} N m/mm³. This elevated wear resistance can be attributed to the optimized thickness and composition of the nitride layer achieved following 12 h of treatment. This enhancement may be ascribed to the presence of a robust layer composed of hard nitrides resulting from an extended period of GN. Among the specimens subjected to nitriding at 550°C, the sample (GN550°C at 24 h) treated for 24 h demonstrates the most pronounced wear resistance, as indicated by its low wear rate value of 0.30×10^{-6} g/m (−0.66507 μm), as shown in Figure 10(c). This superiority is likely attributed to the presence of a substantial nitride layer consisting of hard nitrides formed due to prolonged nitriding at the surface.

As shown in Figure 10(d), at a temperature of 510°C, the GN510°C at 30-h sample exhibits a remarkably low wear rate of 0.05×10^{-6} g/m (−0.53597 μm). The wear resistance is most effectively manifested in the GN510°C at 30-h specimen, possibly attributable to the development of a hard nitride layer approximately 206 μm in thickness formed during the 30-h GN process. This resilient layer markedly augments the sample's wear resistance. The GN545°C at 90-h sample has demonstrated an exceptionally low wear rate of 0.36×10^{-6} g/m (−0.78078 μm), signifying superior wear resistance. This enhanced performance can be ascribed to the extended nitriding duration of 90 h, which likely facilitated the formation of a more homogeneous and well-integrated nitride layer, thereby improving the overall wear characteristics of the material.

The wear volumes of the gas-nitrided specimens at 500°C for 24 h, 510°C for 30 h, 520°C for 12 h, 545°C for 90 h, and 550°C for 24 h under an applied load of 20 N and a sliding speed of 1,909 rpm were measured to be 0.067×10^{-3}, 0.120×10^{-3}, 0.198×10^{-3}, 0.171×10^{-3}, and 0.142×10^{-3} mm³/m for a sliding distance of 3,600 m, respectively.

4 Conclusion

M50 NiL steel specimens subjected to varying temperatures between 500 and 550°C for durations of 8, 12, 24, 20, 30, and 90 h are rigorously examined under GN conditions to ascertain the phase structure, microstructural alterations, wear resistance, corrosion behavior, and microhardness; from these investigations, the principal findings are delineated as follows.

The gas nitride layer comprises a diffusion layer, and subsequent to the nitriding process, phases such as α-FeN, γ-FeN, as well as γ-Fe_3N and Fe_2O_4 are generated on the surface layer of M50 NiL, thereby underscoring the gradual evolution of these phases over time at intermediate temperature ranges. Microhardness measurements of M50 NiL gas nitride specimens at 500°C for a duration of 24 h revealed a value of 1,070 HV, which is approximately five-fold greater than that of the untreated specimen, recorded at 294 HV; this enhancement is likely attributable to the formation of hard compounds like γ-Fe_3N and Fe_3O_4, in conjunction with the expansion of the iron lattice structure. The wear resistance and friction coefficient of M50 NiL gas nitride samples at 500°C for 24 h exhibited the lowest wear rate of 0.16×10^{-6} g/m (−0.34609 μm) and a friction coefficient of 0.2900; conversely, the untreated sample demonstrated a wear rate of 0.52×10^{-6} g/m (−1.08422 μm), accompanied by a COF of 0.5773. The friction coefficient and wear rate of the nitrided specimens are markedly superior to those of the untreated samples. The corrosion resistance characteristics of the M50 NiL nitride sample are considerably enhanced at 500°C for a duration of 24 h, with the specimen exhibiting a corrosion rate of 9.3816 mpy, which is significantly lower than the corrosion rate of 49.577 mpy observed for the

untreated sample. This type of low-pressure GN process can be optimized in the future to obtain effective process parameters.

Funding information: This research was financially supported by research grants from the Aeronautical Research and Development Board, New Delhi. The authors wish to express their gratitude to ARDB for their support of this publication (1957).

Author contributions: All authors have accepted responsibility for the entire content of this manuscript and consented to its submission to the journal, reviewed all the results, and approved the final version of the manuscript. B.V. and K.V.R. designed the experiments, and C.A.K.R. carried them out. B.N.R. developed the model for characterization. C.A.K.R. prepared the manuscript with guidance from all co-authors.

Conflict of interest: Authors state no conflict of interest.

Data availability statement: Data sharing is not applicable to this article as no datasets were generated or analyzed during the current study.

References

[1] Wang N, Liu J. Effect of process parameters on gas nitriding of grey cast iron. Adv Mater Sci Eng. 2013;2013:1–6.
[2] Rana BR, Panchal K. Characterization of gas nitrided 304L stainless steel. Int J Res Appl Sci Eng Technol. 2018;6(9):1–8.
[3] Kochmański P, Nowacki J. Activated gas nitriding of 17-4 PH stainless steel. Surf Coat Technol. 2006;200(22–23):6558–62.
[4] Akhtar SS, Arif AFM, Yilbas BS. Evaluation of gas nitriding process with in-process variation of nitriding potential for AISI H13 tool steel. Int J Adv Manuf Technol. 2009;47(5–8):687–98.
[5] Nam ND, Xuan NA, Van Bach N, Nhung LT, Chieu LT. Control gas nitriding process: A review. J Mech Eng Res Dev. 2019;42(1):17–25.
[6] De Almeida EADS, Milan JCG, Da Costa CE. Acquired properties comparison of solid nitriding, gas nitriding and plasma nitriding in tool steels. Mater Res. 2015;18(1):27–35.
[7] Yang M, Zimmerman C, Donahue D, Sisson RD. Modeling the gas nitriding process of low alloy steels. J Mater Eng Perform. 2012;22(7):1892–8.
[8] Mahmoud HRS, Yusoff SA, Zainuddin A, Hussain P, Ismail M, Abidin K. Effective duration of gas nitriding process on AISI 316L for the formation of a desired thickness of surface nitrided layer. MATEC Web of Conferences. Vol. 13, 2014. p. 04021.
[9] Cegil O, Sen U, Sen S. A comparative study on the corrosion behaviour of gas nitrided and TiAlN coated AISI D2 steel by thermo-reactive diffusion technique. Acta Phys Pol A. 2013;123(2):265–7.
[10] Zhou H, Shi X, Huang Y, Liu X, Li B. Tribological performance of M50-Ag-TiC self-lubricating composites at elevated temperature. J Mater Eng Perform. 2018;27(7):3731–41.
[11] Yeh SH, Chiu LH, Chang H. Effects of gas nitriding on the mechanical and corrosion properties of SACM 645 steel. Engineering. 2011;3(9):942–8.
[12] Xie W, Chen Y, Chen D, Yang Y, Zhang C, Cui G, et al. Low-pressure gas nitriding of AISI 304 austenitic stainless steel: reducing the precipitation of chromium nitrides. Mater Res Express. 2020;7(6):066406.
[13] Reddy GK, Subbaiah R, Sravanthi J, Vafaeva KM. Influence of AISI 304 austenitic stainless steel by aqueous soluted nitriding and gas nitriding. MATEC Web of Conferences. Vol. 392, 2024. p. 01019.
[14] Yuan X, Zhao Y, Li X, Chen L. Effects of gas nitriding temperature on the surface properties of a high manganese TWIP steel. Metals. 2017;7(3):102.
[15] Tang D, Zhang C, Zhan H, Huang W, Ding Z, Chen D, et al. High-efficient gas nitridation of AISI 316L austenitic stainless steel by a novel critical temperature nitriding process. Coatings. 2023;13(10):1708.
[16] Roliński E. Plasma-assisted nitriding and nitrocarburizing of steel and other ferrous alloys. Thermochemical surface engineering of steels. Improving materials performance. Vol. 1, 2015. p. 413–57.
[17] Buzdugan RM, Dan M, Hulka I, Dome M, Feier A, Pascu DR, et al. Corrosion behaviour of duplex treated EN 42CrMo4 steel by gas nitriding and TiAlN PAPVD deposition. Adv Mater Res. 2016;1138:159–64.
[18] Chemkhi M, Retraint D, Roos A, Demangel C. Role and effect of mechanical polishing on the enhancement of the duplex mechanical attrition/plasma nitriding treatment of AISI 316L steel. Surf Coat Technol. 2017;325:454–61.
[19] Townsend DP, Bamberger EN. Surface fatigue life of M50NiL and AISI 9310 gears and rolling-contact bars. J Propuls Power. 1991;7(4):642–9.
[20] Emami M, Ghasemi HM, Rassizadehghani J. Effects of testing temperature and sliding speed on the wear behavior of a low alloy gas nitrided steel. Adv Mater Res. 2011;264–265:1982–7.
[21] Wang B, Sun S, Guo M, Jin G, Zhou Z, Fu W. Study on pressurized gas nitriding characteristics for steel 38CrMoAlA. Surf Coat Technol. 2015;279:60–4.
[22] Zhou YL, Xia F, Xie AJ, Peng HP, Wang JH, Li ZW. A review—Effect of accelerating methods on gas nitriding: Accelerating mechanism, nitriding behavior, and techno-economic analysis. Coatings. 2023;13(11):1846.
[23] Yan G, Lu S, Zhang M, Wang J, Yang X, Zhang Z, et al. Wear and corrosion behavior of P20 steel surface modified by gas nitriding with laser surface engineering. Appl Surf Sci. 2020;530:147306.